Journal of Atomic, Molecular, Condensate & Nano Physics
Vol. 7, No. 2, pp. 83–94, 2020
ISSN 2349-2716 (online); 2349-6088 (print)
Published by RGN Publications

http://www.rgnpublications.com

DOI: 10.26713/jamcnp.v7i2.1407

Research Article

Electron Impact Excitation of Singly Charged Indium Ion

Swati Bharti and Lalita Sharma*

Indian Institute of Technology Roorkee, Roorkee, Uttarakhand 247667, India
***Corresponding author:** lalita.sharma@ph.iitr.ac.in

Abstract. We study electron impact excitation of In^+ using relativistic distorted wave method and report cross sections for 37 transitions among the fine-structure levels of $5s^2$, $5s5p$, $5s5d$, $5s6s$ and $5s6p$ configurations at the scattered electron energies upto 200 eV. The bound state wavefunctions of the target ion are obtained within multi-configuration Dirac-Fock approach. Our calculated oscillator strengths are compared with the results from the NIST database and other theoretical calculations. Cross sections are fitted with an analytical formula and the fitting parameters are made available for their possible applications in plasma modeling.

Keywords. Relativistic distorted waves; Multiconfiguration Dirac-Fock method; Dipole allowed transition; Cross sections; Oscillator strength; Fitting parametres

PACS. 32.80.Cy

Received: April 22, 2020 **Accepted:** June 2, 2020

1. Introduction

Singly charged indium ion has been the subject of various experimental and theoretical studies due to its significant presence in interstellar medium and application in solid state lasers [1–3]. It is also a good candidate for optical frequency precision [4]. Most of the previous work on In^+ is focused on its spectroscopic properties, while inelastic collisions of electrons with In^+ have been subjected to rare investigations. Studies on electron impact excitation of In^+ are required not only for better understanding of its atomic structure, but also to model astrophysical and laboratory plasmas. Theoretical calculations are major source of cross section results since measurements can be very complicated for metal ions due to various technical reasons. Thus, in the present paper we focus on the study of electron impact excitation of In^+ using the RDW method.

Gomonai and co-workers did few experimental studies related to electron collisions with indium ions [5–9]. The most relevant to our present work is their experiment in which Gomonai *et al* [5] reported the effective electron excitation cross-section of In^+ for the resonance transition $5s^2\,{}^1S_0 - 5s5p\,{}^1P_1^\circ$ in the energy range 7–300 eV. The absolute values of these cross-sections were determined by normalizing their measurement at 300 eV energy with Van-Regemorter formula. Smirnov measured excitation cross sections for 123 spectral lines of In^+ at a single electron energy of 30 eV using the extended crossed beam technique [10]. Apart from these measurements, no other theoretical or experimental work has been reported for excitation cross sections of In^+. However, there are several extensive theoretical as well as experimental studies related to spectral properties of In^+. Karlsson and Litzén [11] determined improved wavelengths and energy levels for 54 lines of In^+ using a high-resolution Fourier transform spectrometer. Energy level and hyperfine structures constants of $5s5p\,{}^3P^\circ_{0,1,2}$ and $5s6s\,{}^3S_1$ have been precisely measured by Larkin and Hannaford [4]. They reported transition energy of the forbidden transition $5s^2\,{}^1S_0 - 5s5p\,{}^3P_0^\circ$ at 42275.986(7) cm^{-1} which has been found to be a strong candidate for the optical frequency standard. Peik *et al* performed the laser spectroscopy to measure the hyperfine splitting and isotope shifting for $5s^2\,{}^1S_0 - 5s5p\,{}^3P_1^\circ$ transition at 230.6 nm in In^+ ion [12] for the optical applications. Among theoretical studies Biémont and Zeippen [13] calculated the life time and transition probabilities of singly charged indium ion using relativistic Hartee-Fock approach. Jönsson and Andersson [14] reported extensive data for oscillator strengths and hyperfine structures for a large number of electric dipole transitions of this ion by employing relativistic multiconfiguration Dirac-Hartree-Fock method. Recently, Kramida [15] systemized a detailed list of the best measured wavelengths in the spectra of In^+. In addition, the references to previous experimental and theoretical investigations on spectroscopic properties of In^+ can be found in [15].

From the above discussion it is clear that studies related to electron collisions with In^+ are sparse and will be worthwhile because of their practical applications in various fields. The ground state electronic configurations for In^+ is$[1s^2 2s^2 2p^6 3s^2 3p^6 3d^{10} 4s^2 4p^6 4d^{10}]5s^2$. From here onwards, we will exclude the part of configuration inside square brackets for the sake of brevity. In the present work, we have considered electron impact excitation of the dipole allowed (E1) transitions among fine-structure levels of configurations $5s^2$, $5s5p$, $5s6s$, $5s6p$ and $5s5d$. The wavefunctions of the incoming and outgoing electrons are calculated by solving coupled Dirac equations using RDW approximation [16]. The required bound state wavefunctions of In^+ are obtained within the framework of multi-configuration Dirac-Fock method using GRASP2K [17]. Since the accuracy of the target bound states play major role in determining the collision parameters, we ensure the quality of the ionic wavefunctions by comparing our calculated oscillator strengths with the previously reported calculations [13, 14] and values from the NIST database [18]. Finally, the excitation cross sections for all the 37 transitions are obtained in the range of scattered electron energy from 15 to 200 eV.

In Section 2, we describe RDW method as well as determination of bound state wavefunctions briefly. Results are presented in Section 3, followed by concluding remarks in Sections 4.

2. Theoretical Method

The RDW T-matrix for electron impact excitation of an ion having N electrons and nuclear charge Z from an initial state with total angular momentum J_i to a higher lying state with total angular momentum J_f can be expressed as (atomic units are used throughout)

$$T^{DW}_{J_i \to J_f} = \langle \chi^-_f(1,2,\ldots,N+1)|V - U_f(N+1)|\mathscr{A}\chi^+_i(1,2,\ldots,N+1)\rangle. \tag{2.1}$$

Here V is the interaction of projectile electron with target ion, given by

$$V = -\frac{Z}{r_{N+1}} + \sum_{i=1}^{N} \frac{1}{|r_i - r_{N+1}|}. \tag{2.2}$$

In above equation r_i $(i = 1 \ldots N)$ and r_{N+1} represent the position coordinates of the target and projectile electrons, respectively, with nucleus considered as origin. $U_f(N+1)$ refers to the distortion potential which is chosen to be the spherically symmetric static potential of the target in its final states. $\chi_{i/f}$ denote the product of atomic wavefunction $\Phi_{i/f}$ and projectile electron distorted wavefunction $F^{DW\pm}_{i/f}$ in initial/final states, i.e.,

$$\chi^{\pm}_{i/f}(1,2,\ldots,N+1) = \Phi_{i/f}(1,2,\ldots N)F^{DW\pm}_{i/f,\mu_{i/f}}(k_{i/f},N+1). \tag{2.3}$$

Here $+/-$ sign refer to the incoming/outgoing waves with their respective wavevectors, $k_{i/f}$. $\mathscr{A}$ is the antisymmtrization operator which includes probability of exchange of projectile electron with the target electrons. The spin projections of the incident and scattered electrons are denoted by $\mu_{i/f}$. The procedure of obtaining distorted wavefunctions $F^{DW\pm}_{i/f,\mu_{i/f}}$ can be followed from our previous work [19].

The wavefunctions for initial/final states of In^+ are obtained within multiconfigurational Dirac-Fock (MCDF) approach using GRASP2K code [17]. In this method atomic state functions (ASF) are expressed as linear combinations of configuration state functions (CSFs) with same parity and angular momentum quantum number J. The single particle orbital radial functions and mixing coefficients of CSFs are obtained by solving the Dirac-Coulomb Hamiltonian using self-consistent field method.

After obtaining the bound and continuum state wavefunctions, we can compute T-matrix and finally get the excitation cross section σ using the expression as given below,

$$\sigma(J_i \to J_f) = \frac{4\pi^2}{2(2J_i+1)}\frac{k_f}{k_i}\sum_{\substack{M_i M_f \\ \mu_i \mu_f}} |T^{DW}_{i\to f}|^2 d\Omega. \tag{2.4}$$

3. Results and Discussion

The first step of our calculations involves performing MCDF calculations using GRASP2K program to find wavefunctions of the bound states of In^+. In the present work, we have considered $5s^2$, $5s6s$, $5s5d$, $5s7s$, $5s6d$, $5s8s$, $5p^2$ as even parity configurations and $5s5p$, $5s6p$, $5s4f$, $5s7p$, $5s5f$, $5p5d$, $5s7p$ as odd parity configurations in non-relativistic scheme. These wavefunctions are optimized on the basis of the comparison, as given in Table 1, of our calculated oscillator strengths with the corresponding values from the NIST database [18] as well as other theoretical and experimental studies. Our results are, generally, in good agreement with the the NIST data and lie within the quoted errors, excluding the transitions which have values of oscillator strength less than 10^{-2}.

Table 1. Comparison of our calculated oscillator strengths with the NIST values [18] and other theoretical results [13, 14]. The integers inside parenthesis must be raised to power of 10

Lower state		Upper state		Oscillator strength			
				This work	NIST	Ref [13]	Ref [14]
$5s^2$	$^1S_0$	$5s5p$	$^3P_1^\circ$	2.282(-3)	5.00(-3)	7.300(-3)	4.910(-3)
		$5s5p$	$^1P_1^\circ$	1.803	1.450	1.636	1.560
		$5s6p$	$^3P_1^\circ$	3.293(-5)	1.900(-3)		
		$5s6p$	$^1P_1^\circ$	8.338(-2)	2.700(-3)	2.700(-3)	7.800(-4)
$5s5p$	$^3P_0^\circ$	$5s6s$	$^3S_1$	0.152	0.160	0.176	0.161
		$5s5d$	$^3D_1$	0.982	0.920	0.855	0.877
$5s5p$	$^3P_1^\circ$	$5s6s$	$^3S_1$	0.151	0.160	0.171	0.160
		$5s6s$	$^1S_0$	2.300(-3)	8.000(-4)	3.001(-3)	8.167(-4)
		$5s5d$	$^1D_2$	5.685(-3)	3.100(-3)	1.818(-3)	3.103(-3)
		$5s5d$	$^3D_1$	0.159	0.179	0.208	0.179
		$5s5d$	$^3D_2$	0.614	0.620	0.629	0.620
$5s5p$	$^3P_2^\circ$	$5s6s$	$^3S_1$	0.169	0.162	0.163	0.162
		$5s5d$	$^1D_2$	5.526(-3)	6.000(-3)	8.158(-3)	6.000(-3)
		$5s5d$	$^3D_2$	0.097	0.110	0.118	0.110
		$5s5d$	$^3D_3$	0.660	0.700	0.673	(0.686)
		$5s5d$	$^3D_1$	6.680(-4)	4.500(-3)	0.008	4.520(-3)
$5s5p$	$^1P_1^\circ$	$5s6s$	$^3S_1$	6.340(-4)	1.4(-3)		1.360(-3)
		$5s6s$	$^1S_0$	0.156	0.149	0.227	0.153
		$5s5d$	$^1D_2$	7.725(-3)	4.200(-2)	1.448	3.800(-2)
		$5s5d$	$^3D_1$	4.911(-4)	1.2(-3)	8.548(-4)	1.187(-3)
		$5s5d$	$^3D_2$	1.190(-3)	2.5(-3)	2.482(-3)	2.520(-3)
$5s6s$	$^3S_1$	$5s6p$	$^3P_0^\circ$	0.159	0.149	0.155	0.147
		$5s6p$	$^3P_1^\circ$	0.473	0.440	0.456	0.430
		$5s6p$	$^1P_1^\circ$	6.261(-3)	1.8(-2)	1.800(-2)	1.747(-2)
		$5s6p$	$^3P_2^\circ$	0.814	0.770	0.821	0.763
$5s6s$	$^1S_0$	$5s6p$	$^3P_1^\circ$	1.206(-2)	4.0(-2)	3.974(-2)	3.920(-2)
		$5s6p$	$^1P_1^\circ$	1.268	1.210	1.321	1.190
$5s5d$	$^1D_2$	$5s6p$	$^3P_1^\circ$	1.583(-3)	5.4(-3)		5.240(-3)
		$5s6p$	$^1P_1^\circ$	0.167	0.149		0.146
$5s5d$	$^3D_1$	$5s6p$	$^3P_0^\circ$	7.894(-2)	8.0(-2)		7.767(-2)
		$5s6p$	$^3P_1^\circ$	6.137(-2)	6.000(-2)		5.800(-2)
		$5s6p$	$^1P_1^\circ$	9.825(-4)	-		2.730(-3)
		$5s6p$	$^3P_2^\circ$	3.814(-3)	-		4.200(-3)
$5s5d$	$^3D_2$	$5s6p$	$^3P_1^\circ$	0.111	0.107		0.104
		$5s6p$	$^1P_1^\circ$	1.332(-3)	4.600(-3)		4.480(-3)
		$5s6p$	$^3P_2^\circ$	3.976(-2)	4.0(-2)		3.860(-2)
$5s5d$	$^3D_3$	$5s6p$	$^3P_2^\circ$	0.159	0.157		0.153

The present oscillator strengths also match fairly well with those obtained by Biémont and Zeippen [13] using relativistic Hartree Fock by considering the effect of intravalence configuration interactions on transition probabilities. It can be observed from Table 1 that MCDF calculations of Jönsson and Andersson [14] show better agreement with the NIST results in comparison to ours. This is due to the fact that in ref. [14] the configuration state functions resulting from single excitations of all the core-shells have been considered in the expansion of an atomic state function. The maximum number of relativistic orbitals and CSFs taken are, respectively, 49 and 157000 for even parity states while for odd parity states their respective numbers are 52 and 235000. Thus the spin-polarization, in addition to the core polarization effects via configuration interaction are included more rigorously by Jönsson and Andersson [14]. On the other hand, we have limitations of comprising this kind of large number of CSFs in our RDW method as our main aim is to perform RDW calculations to obtain excitation cross sections using a reasonably accurate set of wavefunctions, which has been finalized on the basis of comparison as shown in Table 1. Since the RDW approximation is a first order perturbation theory, the scattering amplitudes for two electron transitions vanish and hence, the CSFs involving two electron transitions will not contribute. Furthermore, we have ensured in our calculations to include all those CSFs having value of mixing coefficient of the order of 10^{-3}. Thus, the present optimized wavefunction can be counted on to provide accurate cross sections.

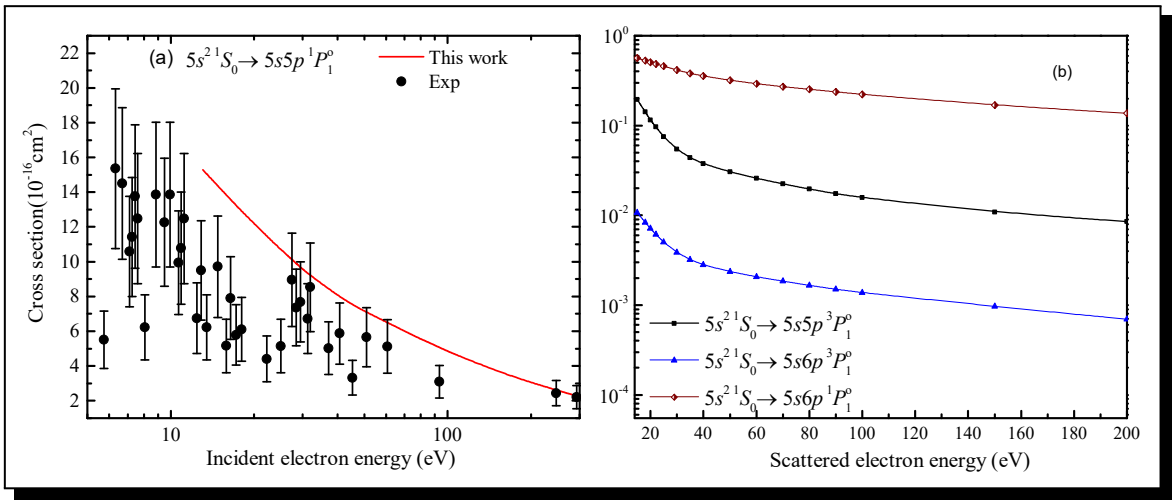

Figure 1. Cross sections for electron impact excitation of the ground $5s^2\,{}^1S_0$ state to the excited (a) $5s5p\,{}^1P^\circ_1$ state compared with the measurements of Gomonai *et al* [5] (b) $5s5p\,{}^3P^\circ_1$ and $5s6p\,{}^{1,3}P^\circ_1$ state

Finally, we have performed RDW calculations for electron impact excitation cross sections of electric dipole transitions among 15 fine-structure levels corresponding to the configurations $5s^2$, $5s5p$, $5s5d$, $5s6s$ and $5s6p$ in In^+. The cross section results are displayed through Figures 1-4. In Figure 1(a) we have compared our results for dipole allowed transition $5s^2\,{}^1S_0 - 5s5p\,{}^1P^\circ_1$ with the only available experimental results for emission cross sections reported by Gomonai *et al* [5] in the electron energy range from 7–300 eV. Although these measurements include cascade effects from higher lying state, we observe that our cross sections are in good agreement with the experimental values at high energies and lie within the uncertainties of the measurements. We notice from Figure 1(b) that cross section curves show a slower logarithmic decline with

respect to the scattered electron energy. This feature is the consequence of the dipole allowed nature of these transitions. Further, it can be seen that the cross sections for same spin transitions are nearly two order of magnitude more than those for spin-change transitions.

Figure 2 presents cross sections for electron impact excitation from excited $5s5p\ ^3P^\circ_{0,1,2}$ and $^1P^\circ_1$ levels to the 6 fine structure levels of $5s6s$ and $5s5d$ configurations. All these transitions show the characteristic feature of the dipole allowed transitions, i.e., slower rate of decrease in cross sections with increasing electron energy. As observed in Figure 1(b), the same spin transitions have greater value of cross sections as compared to spin flip transitions. The relative magnitude of cross sections can further be discerned from their oscillator strengths. We find that more the value of oscillator strength for a particular transition, greater is the value of cross section at a given energy. For example, transition $5s5p\ ^3P^\circ_0 \rightarrow 5s5d\ ^3D_1$ has the largest cross sections among all the 17 transition displayed in Figure 2, owing to maximum value of its oscillator strength.

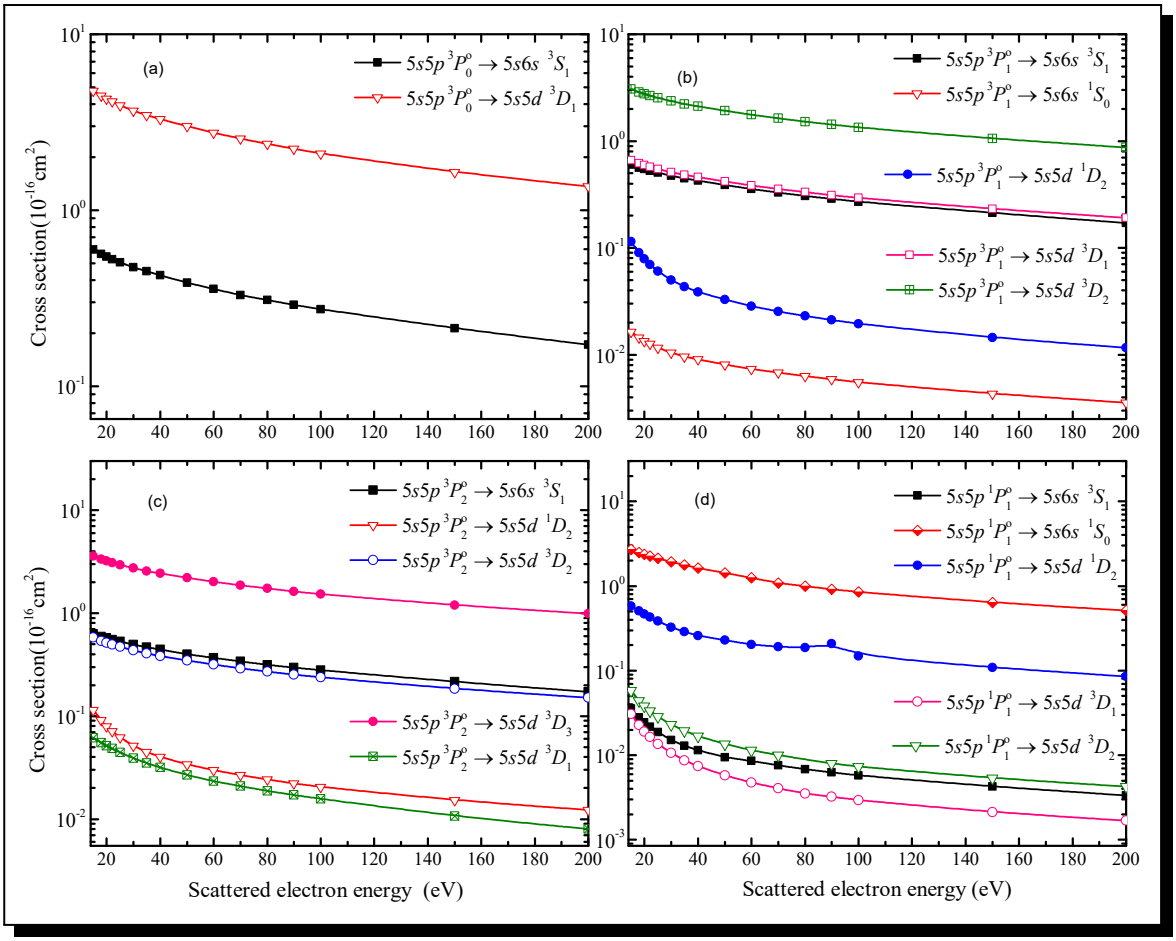

Figure 2. Cross sections for electron impact excitation of the excited states $5s5p\ ^3P^\circ_{0,1,2}$ and $^1P^\circ_1$ to the higher lying fine-structure states $5s6s\ ^3S_1$ and $^1S_0$ as well as $5s5d\ ^3D_{1,2,3}$ and $^1D_2$

Excitation cross section for transitions from $5s6s\ ^3S_1$ and $^1S_0$ states to $5s6p\ ^3P^\circ_{0,1,2}$ and $^1P^\circ_1$ states are depicted in Figure 3. As observed earlier, the increasing order of cross sections can be traced back to oscillator strength for a particular transition as well as to the fact whether or

not the spin change of the state is involved during the transition. Finally, we have shown cross section results for electron impact excitation of $5s5d\ ^3D_{1,2,3}$ and $^1D_2$ states to the higher lying fine-structure states $5s6p\ ^3P^\circ_{0,1,2}$ and $^1P^\circ_1$ in Figure 4. Here again, the behavior of the cross section curves is similar as noticed for other dipole allowed transitions in Figures 1-3. We would like to mention here that in spite of small values of oscillator strengths of these transitions, magnitude of the cross sections is relatively higher in comparison to the cross sections for excitation from the ground state to the farther lying states. This is clearly due to small value of excitation threshold, less than 2 eV, for these transitions.

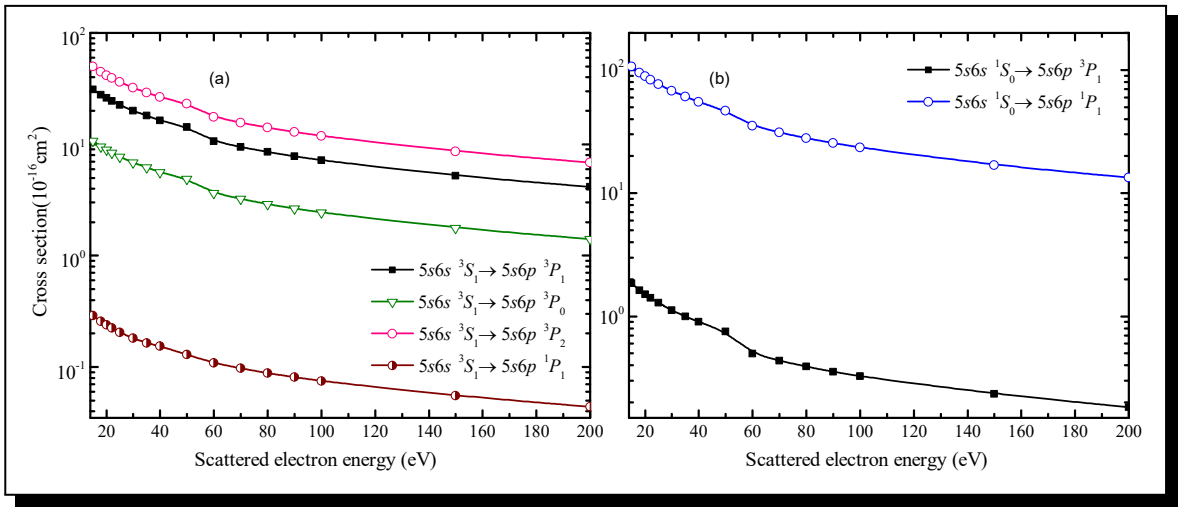

Figure 3. Cross sections for electron impact excitation of the excited states $5s6s\ ^3S_1$ and $^1S_0$ to the higher lying fine-structure states $5s6p\ ^3P^\circ_{0,1,2}$ and $^1P^\circ_1$

In order to make our results available for plasma modeling, we have fitted our calculated cross sections for all the fine-structure transitions using the two analytical expressions. For low to intermediate energy range, the following analytical formula [20] has been employed to fit the cross sections,

$$\sigma(J_i \to J_f) = \frac{\sum_{i=0}^{n} b_i E^i}{c_0 + c_1 E + c_1 E^2}\,. \tag{3.1}$$

Here, incident electron energy E and cross section (σ) are in atomic units. In the above equation b_i, c_0, c_1 and c_2 are the fitting coefficients which are listed in Table 2 for the 37 transitions considered in the present work. Cross section for a given transition can be directly calculated by inserting the fitting coefficients in above expressions. The uncertainty in the fitted cross sections is found to be less than 4%. Further, the cross sections for dipole allowed transitions fall-off as $\ln E/E$ in high energy range of the projectile electron. Therefore, the Bethe-Born form, as given below, is used to fit the cross sections at high energies,

$$\sigma(J_i \to J_f) = \frac{1}{E}(d_0 + d_1 \ln(E)), \tag{3.2}$$

where scattered electron energy E and cross section (σ) are in atomic units. The fitting coefficients d_0 and d_1 are provided in Table 2.

Table 2. The fitting parameters for cross sections of the transitions considered in In^+ ion. The integers inside the parenthesis must be raised to power of 10

Transition	Energy range (eV)	Equation (3.1)							Equation (3.2)	
		b_0	b_1	b_2	b_3	c_0	c_1	c_2	d_0	d_1
$5s^2\ {}^1S_0 \rightarrow 5s5p\ {}^3P_1^\circ$	19.566 – 94.566	1.99336	-2.39449	1.66368	-2.25350(-1)	2.62942	-7.04577	7.62584	1.93120(-1)	1.22700(-2)
$5s^2\ {}^1S_0 \rightarrow 5s5p\ {}^1P_1^\circ$	23.073 – 208.073	3.19393(+1)	3.22066(+1)	-5.19678	2.55760(-1)	-8.39200(-2)	1.81101	-9.19100(-2)	2.84813(+1)	2.47467(+1)
$5s^2\ {}^1S_0 \rightarrow 5s6p\ {}^3P_1^\circ$	27.653 – 162.653	1.64727(+2)	-2.02931(+2)	1.43274(+2)	-1.24176(+1)	1.17932(+4)	-2.52880(+4)	1.57574(+4)	1.58000(-2)	1.62000(-3)
$5s^2\ {}^1S_0 \rightarrow 5s6p\ {}^1P_1^\circ$	28.0567 – 213.057	-1.04724	-7.89800(-2)	1.91631	-1.21080(-1)	8.96390(-1)	-2.88500	2.31498	1.54872	1.03648
$5s5p\ {}^3P_0^\circ \rightarrow 5s6s\ {}^3S_1$	21.574 – 206.574	-3.60576	6.50934	0.56631	-0.03354	-1.26378	1.425	1.62909	1.66480	1.45576
$5s5p\ {}^3P_0^\circ \rightarrow 5s5d\ {}^3D_1$	22.598 – 207.598	7.12479	2.15727(+1)	-1.45064	8.43200(-2)	-1.30800(-1)	1.67915	2.22040(-1)	1.25636(+1)	1.15324(+1)
$5s5p\ {}^3P_1^\circ \rightarrow 5s6s\ {}^3S_1$	21.422 – 206.422	-4.00813	6.85772	7.06570(-1)	-4.30600(-2)	-1.34566	1.33322	1.84244	1.67159	1.43226
$5s5p\ {}^3P_1^\circ \rightarrow 5s6s\ {}^1S_0$	22.099 – 87.099	5.05000(-2)	-2.07650(-1)	3.07360(-1)	-3.08400(-2)	3.04752	-9.99364	9.44487	3.55700(-2)	2.85400(-2)
$5s5p\ {}^3P_1^\circ \rightarrow 5s5d\ {}^1D_2$	21.608 – 106.608	-5.37000(-2)	-9.19100(-2)	5.76010(-1)	-5.62100(-2)	2.31275	-7.43236	6.50492	1.79340(-1)	5.87400(-2)
$5s5p\ {}^3P_1^\circ \rightarrow 5s5d\ {}^3D_1$	22.446 – 207.446	2.36300(-2)	6.03852	-0.22225	1.54200(-2)	-5.98970	2.68015	6.63940(-1)	1.73967	1.62741
$5s5p\ {}^3P_1^\circ \rightarrow 5s5d\ {}^3D_2$	22.453 – 207.453	3.95753	1.48060(+1)	-8.16590(-1)	4.97000(-2)	-1.55020(-1)	1.68838	2.87370(-1)	8.09760	7.31614
$5s5p\ {}^3P_2^\circ \rightarrow 5s6s\ {}^3S_1$	21.091 – 206.091	-3.47966	5.46955	7.21680(-1)	-4.57600(-2)	-1.03275	7.66540(-1)	1.59623	1.75943	1.43746
$5s5p\ {}^3P_2^\circ \rightarrow 5s5d\ {}^1D_2$	21.278 – 106.278	-4.31600(-2)	-7.40800(-2)	5.51560(-1)	-5.33300(-2)	1.94711	-6.47262	5.93886	1.84750(-1)	6.50000(-2)
$5s5p\ {}^3P_2^\circ \rightarrow 5s5d\ {}^3D_2$	22.122 – 207.122	1.51514	5.07177	-2.10570(-1)	1.31300(-2)	-3.22900(-1)	3.13561	6.69390(-1)	1.51894	1.22756
$5s5p\ {}^3P_2^\circ \rightarrow 5s5d\ {}^3D_3$	22.132 – 207.132	3.17316	1.62246(+1)	-6.86770(-1)	4.49100(-2)	-1.82870(-1)	1.49813	3.27310(-1)	9.43521	8.21913
$5s5p\ {}^3P_2^\circ \rightarrow 5s5d\ {}^3D_1$	22.115 – 157.115	9.19160(-1)	2.55340(-1)	1.60800(-1)	-1.60100(-2)	1.12685	2.91659	3.13609	1.72650(-1)	2.27300(-2)
$5s5p\ {}^1P_1^\circ \rightarrow 5s6s\ {}^3S_1$	17.915 – 202.915	-4.44019(+1)	5.11148(+2)	9.01417(+2)	-6.41894(+1)	9.71519(+3)	-3.76227(+4)	4.68744(+4)	5.27500(-2)	1.78200(-2)
$5s5p\ {}^1P_1^\circ \rightarrow 5s6s\ {}^1S_0$	18.593 – 203.593	-6.22254	1.37097(+1)	-8.34310(-1)	9.25900(-2)	-4.23820(-1)	5.00810(-1)	7.89160(-1)	7.21992	3.19046
$5s5p\ {}^1P_1^\circ \rightarrow 5s5d\ {}^1D_2$	18.102 – 83.102	2.03876	5.74180(-1)	1.66565	9.37200(-2)	1.25950	-2.37539	4.21352	1.37332	4.47630(-1)
$5s5p\ {}^1P_1^\circ \rightarrow 5s5d\ {}^3D_1$	18.939 – 203.939	-2.30156	4.39506	3.40230(-1)	2.10000(-3)	4.19678(+1)	-1.66219(+2)	1.69461(+2)	3.06700(-2)	6.34000(-3)
$5s5p\ {}^1P_1^\circ \rightarrow 5s5d\ {}^3D_2$	18.946 – 73.946	4.20910(-1)	1.69200(-2)	–	–	-2.43545	6.76446	-4.01810(-1)	6.97700(-2)	2.05900(-2)
$5s6s\ {}^3S_1 \rightarrow 5s6p\ {}^3P_0^\circ$	16.641 – 51.641	5.47249	-1.55789	-3.23820(-1)	–	3.76600(-2)	1.76270(-1)	-8.19400(-2)	2.31722(+1)	6.88411
$5s6s\ {}^3S_1 \rightarrow 5s6p\ {}^3P_1^\circ$	16.665 – 41.665	5.46097	1.02834(+1)	–	–	3.40000(-3)	1.22110(-1)	7.32800(-2)	6.78170(+1)	2.03775(+1)

Contd. Table 2

$5s6s$	$^3S_1 \rightarrow 5s6p$	$^1P_1^\circ$	17.069 – 202.069	-1.18820	4.80634	-2.30590(-1)	2.86100(-2)	-1.14052	2.27505	3.53414	6.94360(-1)	2.26570(-1)
$5s6s$	$^3S_1 \rightarrow 5s6p$	$^3P_2^\circ$	16.729 – 51.729	1.77275(+1)	-3.97013	-1.05171	–	2.60500(-2)	1.25180(-1)	-5.15900(-2)	1.10974(+2)	3.44284(+1)
$5s6s$	$^1S_0 \rightarrow 5s6p$	$^3P_1^\circ$	15.987 – 40.987	2.40360	1.32665	-1.00740(-1)	–	5.62400(-2)	6.48390(-1)	1.15700(-1)	3.34620	7.19440(-1)
$5s6s$	$^1S_0 \rightarrow 5s6p$	$^1P_1^\circ$	16.391 – 51.391	-5.30440	4.39856(+1)	3.68506(+1)	-7.49463	3.84000(-3)	-3.51800(-2)	2.85700(-1)	2.27408(+2)	6.20001(+1)
$5s5d$	$^1D_2 \rightarrow 5s6p$	$^3P_1^\circ$	16.478 – 201.478	4.45820(-1)	1.51920	3.76300(-2)	-8.12752(-4)	-2.24880(-1)	2.89709	3.07780	3.34910(-1)	9.01600(-2)
$5s5d$	$^1D_2 \rightarrow 5s6p$	$^1P_1^\circ$	16.882 – 201.882	-5.13680(-1)	2.35127(+1)	6.95020(-1)	-1.05000(-2)	-6.78600(-2)	3.90530(-1)	6.72040(-1)	2.27381(+1)	7.83741
$5s5d$	$^3D_1 \rightarrow 5s6p$	$^3P_0^\circ$	15.617 – 60.617	-1.07492(+1)	1.86570(+1)	3.22486	-3.86220(-1)	-1.98900(-2)	-1.57200(-1)	3.67990(-1)	5.52305(+1)	1.16315(+1)
$5s5d$	$^3D_1 \rightarrow 5s6p$	$^3P_1^\circ$	15.641 – 60.641	-7.34721	1.30787(+1)	2.26353	-2.69520(-1)	-1.89300(-2)	-1.44720(-1)	3.51030(-1)	4.04277(+1)	8.66127
$5s5d$	$^3D_1 \rightarrow 5s6p$	$^3P_2^\circ$	15.705 – 100.705	-2.96013	5.48459	4.43170(-1)	-4.36500(-2)	-1.22410(-1)	-5.56750(-1)	1.53058	3.38535	6.00850(-1)
$5s5d$	$^3D_1 \rightarrow 5s6p$	$^1P_1^\circ$	16.045 – 201.045	-4.08150(-1)	1.94433	1.34020(-1)	-6.47000(-3)	-4.59070(-1)	2.66700(-1)	5.26069	3.19360(-1)	7.39200(-2)
$5s5d$	$^3D_2 \rightarrow 5s6p$	$^3P_1^\circ$	15.634 – 80.634	1.85480(+1)	-2.66365	1.10101(+1)	-8.88990(-1)	4.63800(-2)	1.93740(-1)	-3.18300(-2)	7.45894(+1)	1.58943(+1)
$5s5d$	$^3D_2 \rightarrow 5s6p$	$^3P_2^\circ$	15.698 – 60.698	-5.67210	1.04743(+1)	1.68231	-1.93150(-1)	-2.70400(-2)	-1.77710(-1)	4.61870(-1)	2.39480(+1)	5.27641
$5s5d$	$^3D_2 \rightarrow 5s6p$	$^1P_1^\circ$	16.038 – 201.038	-7.49130(-1)	2.63119	1.80230(-1)	-8.69000(-3)	-4.51450(-1)	-1.69830(-1)	5.14794	4.41010(-1)	1.06100(-1)
$5s5d$	$^3D_3 \rightarrow 5s6p$	$^3P_2^\circ$	15.688 – 60.688	-1.37211(+1)	2.52997(+1)	4.44060	-5.26770(-1)	-1.55900(-2)	-1.12410(-1)	2.87940(-1)	9.48479(+1)	2.10234(+1)

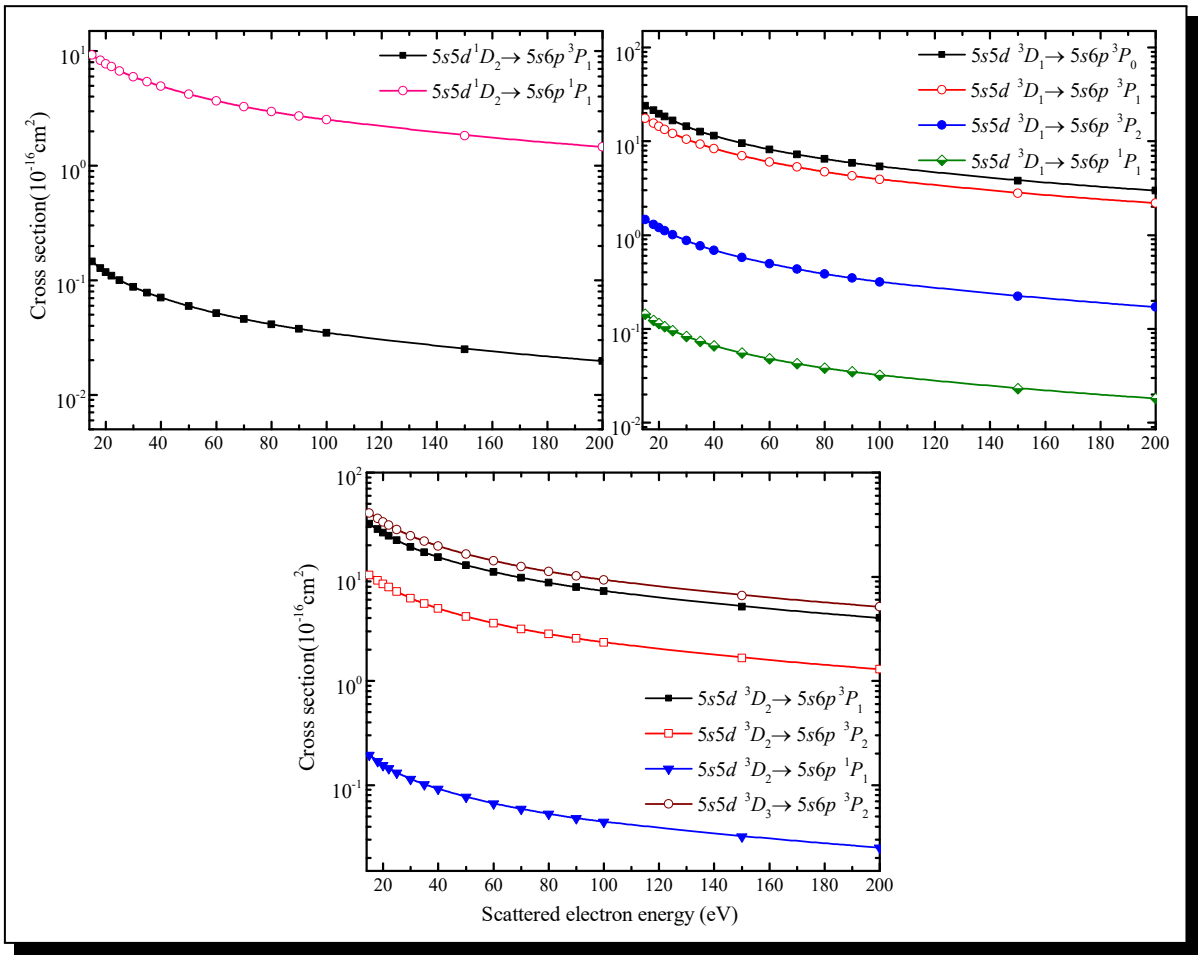

Figure 4. Cross sections for electron impact excitation of the excited states $5s5d\,^3D_{1,2,3}$ and $^1D_2$ to the higher lying fine-structure states $5s6p\,^3P_{0,1,2}$ and $^1P_1^\circ$

4. Conclusions

We have studied electron impact excitation of singly charged indium ion using RDW method. The cross section calculations are performed for dipole allowed fine-structure transitions among the states arising from the configurations $5s^2$, $5s5p$, $5s5d$, $5s6s$ and $5s6p$ in the scattered electron energy range of 15-200 eV. We have provided a detailed comparison of our calculated oscillator strengths for these transitions with the values listed in the NIST database and other theoretical results and found an overall good agreement. This ensures the quality of bound state wavefunctions employed in our calculations as well as reliability of the cross sections reported here. Cross sections for the transition $5s^2\ ^1S_0 \rightarrow 5s5p\ ^1P_1^\circ$ are compared with the measurements of Gomonai *et al* [5] and a good agreement is found at high energies. Unfortunately, there are no other theoretical and experimental results available to compare with our calculated cross sections for other transitions. Finally, we have provided fitting of our cross sections using two analytical expressions based on low and high energy ranges of the incident electron. We hope our results will be useful for plasma modelers and stimulate more work on electron induced processes in singly charged indium ions.

Acknowledgements

Swati Bharti would like to acknowledge Ministry of Human Resources and Development (MHRD) India for the award of a research fellowship. Lalita Sharma is grateful to the Department of Science & Technology (DST) India and the Council of Scientific and industrial Research (CSIR), New Delhi, India for providing research grants.

Competing Interests

The authors declare that they have no competing interests.

Authors' Contributions

All the authors contributed significantly in writing this article. The authors read and approved the final manuscript.

References

[1] F. Paschen and J. S. Campbell, Das erste Funkenspektrum des Indiums in II, *Annalen der Physik* **31** (1938), 29, DOI: 10.1002/andp.19384230103.

[2] C. E. Moore, *Atomic Energy Levels*, Volume **3** (1958), p. 67, National Bureau of Standards, Washington DC, `https://apps.dtic.mil/dtic/tr/fulltext/u2/a280279.pdf`.

[3] E. V. Ovcharenko, A. I. Imre, A. N. Gomonai and Yu. I. Hutych, Emission cross-sections of the In^{2+} ion VUV laser transitions at electron–In^{+} ion collisions, *Journal of Physics B: Atomic, Molecular and Optical Physics* **43** (2010), 175206, DOI: 10.1088/0953-4075/43/17/175206.

[4] P. L. Larkins and P. Hannaford, Precision energies and hyperfine structures of the $5s5p\ ^3P^0_{0,1,2}$ and $5s6s\ ^3S_1$ levels in In II, *Zeitschrift für Physik D Atoms, Molecules and Clusters* **27** (1993), 313 – 320, DOI: 10.1007/BF01437462.

[5] A. Gomonai, E. Ovcharenko, A. Imre and Yu. Hutych, Peculiarities of the electron-impact excitation of single-charged indium ion, *Nuclear Instruments and Methods in Physics Research Section B: Beam Interactions with Materials and Atoms* **233** (2005), 250 – 254, DOI: 10.1016/j.nimb.2005.03.116.

[6] A. Gomonai, E. Ovcharenko, A. Imre and Yu. Hutych, Influence of subvalence nd^{10} shell on the excitation of resonance lines of Al^{+} subgroup ions, *Publications of the Astronomical Observatory of Belgrade* **84** (2008), 119 – 122, `http://publications.aob.rs/84/pdf/119-122.pdf`.

[7] A. N. Gomonai, A. I. Imre, E. V. Ovcharenko and Yu. I. Hutych, Near-threshold excitation of the resonance λ 158.6 nm line in electron-indium ion collisions, *Journal of Physical Studies* **13**(2) (2009), 2301, DOI: 10.1088/1742-6596/194/6/062012.

[8] A. N. Gomonai, A. I. Imre, E. V. Ovcharenko and Yu. I. Hutych, Electron-impact excitation of $4d95s^2\ ^2D \rightarrow 4d^{10}5p\ ^2P$ laser transitions in In^{2+} ion from the ground state of In^{+} ion, *Journal of Physics: Conference Series* **194** (2009), 062012, DOI: 10.1088/1742-6596/194/6/062012.

[9] A. N. Gomonai, Yu. I. Hutych, A. I. Gomonai, Emission cross sections for spectral lines transiting from the In^{2+} lower laser $4d^{10}5p\ ^2P_{1/2,3/2}$ states excited by electron impact on the In^{+} ion, *Nuclear Instruments and Methods in Physics Research Section B: Beam Interactions with Materials and Atoms* **311** (2013), 37 – 41, DOI: 10.1016/j.nimb.2013.06.002.

[10] Y. M. Smirnov, Excitation of a singly charged indium ion by electron impact, *Optics and Spectroscopy* **108** (2010), 677 – 684, DOI: 10.1134/S0030400X10050036.

[11] H. Karlsson and U. Litzén, Hyperfine constants, revised wavelengths and energy levels in In I and In II derived by Fourier transform spectroscopy, *Journal of Physics B: Atomic, Molecular and Optical Physics* **34** (2001), 4475, DOI: 10.1088/0953-4075/34/22/315.

[12] E. Peik, G. Hollemann and H. Walther, Laser cooling and quantum jumps of a single indium ion, *Physical Review A* **49** (1994), 402, DOI: 10.1103/PhysRevA.49.402.

[13] E. Biémont and C. J. Zeippen, Lifetimes and transition probabilities in In II, *Atomic Data and Nuclear Data Tables* **72** (1999), 101 – 125, DOI: 10.1006/adnd.1999.0810.

[14] P. Jönsson and M. Andersson, Spectral properties of In II from MCDHF calculations, *Journal of Physics B: Atomic, Molecular and Optical Physics* **40** (2007), 2417, DOI: 10.1088/0953-4075/40/12/016.

[15] A. Kramida, Critically evaluated energy levels and spectral lines of singly ionized indium (In II), *Journal of Research of the National Institute of Standards and Technology* **118** (2013), 52 – 104, DOI: 10.6028/jres.118.004.

[16] P. Jönsson, X. He, C. Froese Fischer and I. P. Grant, The grasp2K relativistic atomic structure package, *Computer Physics Communications* **177** (2007), 597 – 622, DOI: 10.1016/j.cpc.2007.06.002.

[17] P. Jönsson, G. Gaigalas, J. Bieroń, C. Froese Fischer and I. P. Grant, New version: Grasp2K relativistic atomic structure package, *Computer Physics Communications* **184** (2013), 2197 – 2203, DOI: 10.1016/j.cpc.2013.02.016.

[18] NIST Atomic Spectra Database, `www.nist.gov/pml/data/asd.cfm`, DOI: 10.18434/T46C7N.

[19] L. Sharma, A. Surzhykov, R. Srivastava and S. Fritzsche, Electron-impact excitation of singly charged metal ions, *Physical Review A* **83** (2011), 062701 DOI: 10.1103/PhysRevA.83.062701.

[20] S. Gupta, L. Sharma and R. Srivastava, Electron-impact excitation of Xe^+ and polarization of its subsequent emissions, *Journal of Quantitative Spectroscopy and Radiative Transfer* **219** (2018), 7 – 22, DOI: 10.1016/j.jqsrt.2018.07.014.